

Solution enthalpy of hydrogen in fourth row elements: Systematic trends derived from first principles

U. Aydin,* L. Ismer, T. Hickel, and J. Neugebauer

Max-Planck Institut für Eisenforschung, Max-Planck-Straße 1, D-40237 Düsseldorf, Germany

(Received 14 December 2011; revised manuscript received 19 January 2012; published 30 April 2012)

Based on first-principles calculations, we identify a master curve for the solution enthalpy of H in fourth row elements including all 3d transition metals. Assuming nonmagnetic fcc crystal structures, we find two different classes of materials with either the octahedral or the tetrahedral interstitial site being preferred by hydrogen. An interaction radius for H in octahedral site of $\approx 0.7 \text{ \AA}$ ($\approx 0.4 \text{ \AA}$ for H in tetrahedral site) turns out to be a characteristic value for which the chemical interaction energy has an optimum for all studied elements.

DOI: [10.1103/PhysRevB.85.155144](https://doi.org/10.1103/PhysRevB.85.155144)

PACS number(s): 61.72.jj, 71.20.Be, 82.30.Rs

I. INTRODUCTION

The ability of hydrogen to penetrate into metals has been demonstrated first for Pd in 1866.¹ Since the beginning of the 20th century, it is known that the presence of hydrogen can lead to serious material failures in transition metals, a prominent example is the infamous hydrogen embrittlement in steels.² These observations triggered long-standing research activities to gain precise knowledge about the fundamental mechanisms behind hydrogen solution in metals. The resulting theoretical and experimental studies addressed hydrides and hydrogen soluble systems for various hydrogen concentrations.

For hydrides of a few intermetallic and metallic compounds, some empirical laws could be determined.^{3–6} In contrast to this, such laws are largely missing on the opposite concentration regime, i.e., on the dilute H regime. Nevertheless, there is a large number of metals such as steels that do not form bulk hydrides.⁷ For these materials for which the incorporation of hydrogen is often critical with respect to mechanical properties, much less is known about systematic trends. Two rather general concepts are the *proton model* (the electron of the H atom fills states of the host metal, yielding a positively charged H state) and the *anion model* (low-lying hydrogen states empty states of the host metal, yielding a negatively charged H state). Later Nørskov and Besenbacher published an effective medium theory and self-consistent model calculations from which they came to the conclusion that the heat of solution (and other properties) of dilute hydrogen containing metallic systems is strongly correlated to the electron density at the interstitial site and the *d*-band filling of the host metal.⁸

Experiments with hydrogen-charged austenitic steels (up to 5 at.% H) indicated that interstitial hydrogen influences the electronic structure of the host and yields an increase of the conductivity with hydrogen concentration. Further, the density of conduction electrons is higher in hydrogen occupied interstitial sites.⁹

With the development of further semiempirical models, a better understanding of the mechanisms of hydrogen diffusion and solution in transition metals has been developed.^{10–12} These models have, e.g., been used by Griessen to estimate the hydrogen solution enthalpy ΔH in metals. Recent *ab initio* studies on H in Fe and Mn showed a strong influence of the metal lattice constant on the solution enthalpy.¹³ A detailed

analysis showed that differences in the solubility between these two materials can solely be explained by changes in the host lattice constants and subsequently with changes in the interstitial volume.

In the present paper, our aim is to generalize this finding for pure systems and find a computationally inexpensive DFT approach to predict hydrogen solubility from physical bulk parameters also for more complex systems. Accordingly, chemical trends for the hydrogen solution were studied systematically, separating them from atomic effects (e.g., crystal type or magnetism). In particular, we studied fourth row elements of the periodic system from K up to Ge under comparable conditions (pure elements, no magnetism, identical fcc-lattice structure) at 0 K. Our discussion includes a critical *ab initio* evaluation of the parameters introduced by Griessen in his semiempirical approach. The calculations have been done by assuming a dilute limit for hydrogen in the bulk metal and neglecting the effects of H-H interactions on the hydrogen solution enthalpy. We have considered both high-symmetry interstitial sites (o-site and t-site) for hydrogen in these material systems. Furthermore, the effect of zero point vibration has been taken into account.

II. METHODOLOGY

A. Solution enthalpy and solubility of H in metals

Commonly, it is assumed that the hydrogen containing metallic phase is in thermodynamic equilibrium with a surrounding atmosphere of hydrogen molecules, expressed by

$$\mu_{\text{H}}^{\text{g}}(\text{H}_2 \text{ gas}) = \mu_{\text{H}}^{\text{M}}(\text{in M}). \quad (1)$$

Here, $\mu_{\text{H}}^{\text{g}}$ is the chemical potential of a hydrogen atom in a hydrogen molecule and $\mu_{\text{H}}^{\text{M}}$ the chemical potential of atomic hydrogen dissolved in the host metal. Under the assumption that the concentration of hydrogen in the metal is small, Sievert's law

$$c_{\text{H}} = \sqrt{\frac{p}{p_0}} e^{\frac{\Delta S}{k_B}} e^{-\frac{\Delta H}{k_B T}} \quad (2)$$

can be derived (for details, see Ref. 14). Here, T is the temperature, p is the pressure, p_0 is a reference pressure (in general, $p_0 = 1 \text{ atm}$), and k_B the Boltzmann constant. The nonconfigurational entropy of formation ΔS , which is assumed not to change with temperature T , and the solution

enthalpy ΔH are thermodynamic parameters.¹² The key quantity in Eq. (2) is the solution enthalpy ΔH .

B. Predicting solution enthalpy: Griessen's empirical model

During the incorporation of a single hydrogen atom into a metallic matrix, a heat δQ is released.¹⁴ We relate this quantity to quantities accessible by *ab initio* calculations noting that δQ is in an isothermal/isobaric process equal to the change of enthalpy ΔH of the metal-hydrogen system after hydrogen solution:

$$\delta Q = \Delta H = H_{\text{MH}}(p) - H_{\text{M}}(p) - \frac{1}{2}H_{\text{H}_2}(p). \quad (3)$$

Here, H_{MH} is the enthalpy of the metal-hydrogen system and H_{M} is the enthalpy of the pure system. The last part of the equation is the enthalpy of the hydrogen molecule for which we take the enthalpy of a H_2 molecule at zero pressure $p = 0$ as a reference, thus $\frac{1}{2}H_{\text{H}_2}(p = 0) = \mu_{\text{H}}(p = 0)$.

Using the thermodynamic relation $H = U + pV$ for the enthalpy, Eq. (3) leads to

$$\Delta H(p) = \Delta U(p) + pV_{\text{H}}(p) - \mu_{\text{H}}(p = 0), \quad (4)$$

with the pressure-dependent excess volume $V_{\text{H}}(p) = V_{\text{MH}}(p) - V_{\text{M}}(p)$, and the internal energy difference $\Delta U(p) = U_{\text{MH}}(p) - U_{\text{M}}(p)$. Taking the derivative,

$$\frac{\partial \Delta H(p)}{\partial p} = \frac{\partial \Delta U(p)}{\partial p} + V_{\text{H}}(p) + p \frac{\partial V_{\text{H}}(p)}{\partial p}, \quad (5)$$

and employing the fundamental relation $\frac{\partial U}{\partial p} = -p \frac{\partial V}{\partial p}$, one obtains

$$\frac{\partial \Delta H(p)}{\partial p} = V_{\text{H}}(p), \quad (6)$$

which is a fundamental relation between the H induced excess volume V_{H} and the solution enthalpy ΔH (Griessen *et al.*^{11,15}). With the definition for the bulk modulus,

$$B = -V \frac{\partial p}{\partial V}, \quad (7)$$

Eq. (5) is equivalent to¹²

$$\frac{\partial \Delta H(p)}{\partial \ln V_{\text{M}}(p)} = -B(p)V_{\text{H}}(p). \quad (8)$$

For H in transition metals, Griessen *et al.*¹¹ showed that the solution enthalpy strongly depends on the electronic structure of the host metal. As a quantitative measure of the electronic structure, the difference $\Delta E = E_{\text{F}} - E_{\text{s}}$ between the Fermi energy E_{F} and the energy at the center of the lowest conduction band E_{s} was used. In a subsequent study (Ref. 12), he extended this model by taking also the *d-d* band overlap W_{d} and the distance of the hydrogen atom to its nearest-neighboring metal atoms R_j into account:

$$\Delta H = \alpha \Delta E W_{\text{d}}^{1/2} \sum R_j^{-4} + \beta. \quad (9)$$

Here, W_{d} and ΔE are general properties of the host metal. The distances R_j depend on the local configuration.¹² The constants α and β are fitting parameters. This semiempirical model helps to understand how the hydrogen concentration in transition metals is related to specific material-dependent quantities.

A drawback of this and other previous models is their dependence on experimental input data. As a consequence, it is hard to distinguish between different physical effects and to derive the dependence of the solution enthalpy on simple parameters. It is therefore unclear if relations constructed from a certain set of experimental data can also be extended to other materials not considered before. For a deeper and more systematic understanding of the electronic and elastic interactions of hydrogen in metallic systems, *ab initio* methods have the clear advantage that they are universal and solely based on quantum-mechanical principles. This allows a systematic evaluation of the empirical laws and a fundamental understanding of the underlying mechanisms.

C. *Ab initio* description

In order to determine all the contributions to the pressure-dependent solution enthalpy in Eq. (3), we fitted our *ab initio* data to the Murnaghan equation of state for energy.¹⁶ Since H is the lightest element in the periodic table, quantum-mechanical effects in the H motion have to be taken into account. The excess zero-point energy is defined as

$$E^{\text{vib,tot}} = \frac{1}{2}\hbar \left(\sum_j^{3(N+x)} \omega_j^{\text{MH}} - \sum_j^{3N} \omega_j^{\text{M}} - \frac{1}{2} \sum_j^{3x} \omega_j^{\text{H}_2} \right), \quad (10)$$

where the ω_j denote the phonon frequencies of the corresponding systems. The first part of Eq. (10) describes the energy, related to vibrations of the hydrogen-metal system. The second part expresses the energy of the unperturbed (i.e., H-free) system. The third part describes the energy of an oscillating H_2 molecule. In order to obtain these frequencies, we use the harmonic approximation. The actual calculation is performed in two different ways, the Einstein method and the calculation of the full dynamical matrix, respectively. In the Einstein method, which is a computationally inexpensive method, only the hydrogen atom is displaced in three different orthonormal directions. For each of the three directions, the resulting energy versus displacement curve is fitted with a second-order polynomial. The second derivative of the fit is a constant term a , which determines the frequency ω_{H} of the hydrogen atom with the mass m through the relation $\omega_{\text{H}} = \sqrt{2a/m}$.

The more accurate but computationally also much more demanding second approach is calculating the full dynamical matrix, i.e., displacing all atoms. The dynamical matrix is obtained by displacing the atoms by 0.008 Å out of the equilibrium position.¹⁷

As mentioned before, we assume hydrogen to be in the dilute limit ($x \ll N$). In order to evaluate the influence of possible H-H interactions on the solution enthalpy, we performed careful supercell convergence checks for two (with respect to the filling of their 3*d* shells) different 3*d* elements, namely, Ti and Cu. The experimental value for the solution enthalpy for H in the investigated elements (excluding Ge) is in the range of 1.5 eV. We aim at a total error for the solution enthalpy of less than 10% of this value, i.e., the targeted error should be below 0.15 eV. It turned out that in the fcc bulk material, a $2 \times 2 \times 2$ supercell consisting of 32 metal atoms, is sufficient to guarantee an error of <0.05 eV.

All our *ab initio* results have been obtained from DFT calculations using PAW pseudo-potentials¹⁸ implemented in VASP.¹⁹ For the description of electronic exchange and correlation, we have used the GGA-PBE functional,²⁰ yielding an additional error that cannot be quantified. The numerical error due to the choice of a plane-wave cutoff energy of 300 eV and 6912 k points for the sampling of the Brillouin zone (corresponding to a $6 \times 6 \times 6$ Monkhorst-Pack mesh)²¹ is sufficiently small to ensure (besides our energy criterion) an error in the bulk modulus of less than 1 GPa. We have used a Methfessel-Paxton scheme²² with electronic smearing of 0.1 eV. The relaxation of atoms has been performed with a second-order quasi-Newton method. Convergence checks of the solution enthalpy have shown that the numerical error due to k -point sampling and cutoff energy is below 0.02 eV.

III. RESULTS

A. Comparison with experiments

As mentioned above, all our *ab initio* calculations are performed for nonmagnetic (NM) fcc crystal structures. This allows to separate chemical trends from structure and magnetic interactions. The approach is also motivated by the interest in understanding the effect of the local chemical environment on the H solution enthalpy in an fcc alloy. The locally enriched impurity atoms do not change the lattice structure of the host matrix if their concentration is small.

Figure 1 compiles our *ab initio* data and experiment. As can be seen, the experimental data for the $3d$ elements nicely agree with our DFT results. The figure also nicely shows that chemical trends become much more apparent if consistently NM-fcc structures are assumed rather than

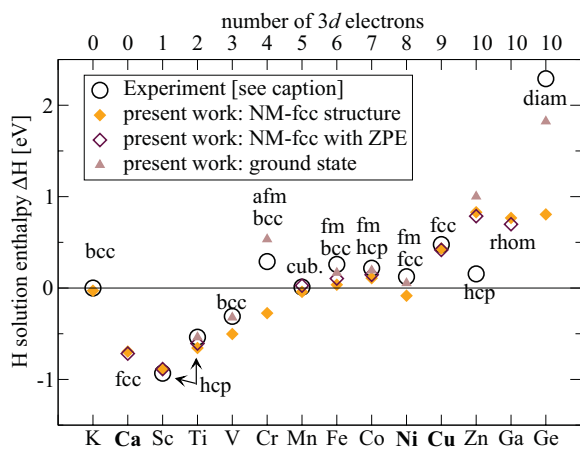


FIG. 1. (Color online) Solution enthalpies of H in $3d$ elements. Circles: Experimental data cited in Ref. 23: K and Sc (see Ref. 24), Ti (see Ref. 25), V and Cu (see Ref. 26), Cr, Mn, Fe, and Co (see Ref. 27), Ni (see Ref. 28), Zn (see Ref. 29), and Ge (see Ref. 30). Filled diamonds: *ab initio* results for $3d$ elements assuming NM-fcc structures. Open diamonds: *ab initio* results including zero-point energy (ZPE) in NM fcc structure. Filled triangles: *ab initio* results for $3d$ elements in their ground state ($T = 0$ K) stable structure, as indicated by the label. The *ab initio* results always refer to the energetically most favorable interstitial site. Bold elements indicates fcc structure for the ground state.

changing a complete set of parameters. Prominent examples are Cr, Ga, or Ge. Finally, we note that zero-point vibrations have little effect on the results.

For the transition metals, we observe a clear dependence of ΔH on the filling of the outer d shell, beginning with one electron in the case of Sc and a filled shell for Cu. Since we observe an increase with the filling of the $3d$ shell, these electrons have apparently a systematic direct or indirect effect on the solution enthalpy. An indirect effect might be a change in the lattice constant, which (indirectly) affects via the interstitial volume the solution enthalpy. In order to discriminate between direct and indirect effects, the lattice constants of the elements have to be taken into account. Previous studies¹¹ as well as our own investigations¹³ have already indicated that apart from the chemical structure of the host lattice, the distance of the interstitial to its next neighboring metallic atom is a decisive parameter controlling H solubility. For example, H solubility increases when alloying Fe with Mn or C, which both expand the Fe lattice. Specifically, a linear relation between the interstitial Voronoi volume and the solubility of hydrogen at the corresponding site has been observed that is almost independent of the chemical environment.¹³

B. Solution enthalpy as a function of the lattice constant

In order to check if such volume effects can be generalized, we replot the solution enthalpies of Fig. 1 as a function of the lattice constant (see Fig. 2). In addition, we systematically varied the volume for each of the studied $3d$ elements around the equilibrium lattice constant, corresponding to an application of hydrostatic pressure.

Since the solution enthalpy in Eq. (2) is a function of pressure, the enthalpy difference between the metal-hydrogen and the metal systems described in Eq. (3) have been calculated at the same pressure. We observe, however, that the volume dependent trends are more clear if we plot the solution enthalpy with respect to the lattice constant instead of pressure. In Fig. 2, the resulting solution enthalpy is shown if H is placed separately in an octahedral [o-site, Fig. 2(a)] and in a tetrahedral site [t-site, Fig. 2(b)]. The derivative for the change, as a function of the volume, is provided in Figs. 2(c) and 2(d), respectively. We notice two interesting effects: (i) the solution enthalpy and, in particular, its slope follow closely an universal master curve. This curve is largely independent of the specific host element. For H in an o-site (t-site), the minimum of the solution enthalpy is at a lattice constant of 4.6 Å (5.5 Å). The occurrence of a minimum indicates the occurrence of competing repulsive and attractive interactions. The volume dependence can be approximately fitted by the following functional dependence $\Delta H(a_{\text{lat}}) = \alpha \exp(-a_{\text{lat}}) - \beta(1/a_{\text{lat}})$ [see red line in Fig. 5(b)]. (ii) For elements with almost the same lattice constant (e.g., Ti and Zn or Fe and Cu), in some cases a constant shift in H solubility is observed. The slope (derivative) remains, however, almost unchanged.

In addition to the solution enthalpy, the *ab initio* approach provides the bulk modulus and the excess volume for a wide range of chemical elements and lattice constants (pressures). This allows to check the performance of the analytical relation provided in Eq. (8). Since in this expression the derivative of the solution enthalpy with respect to the logarithm of

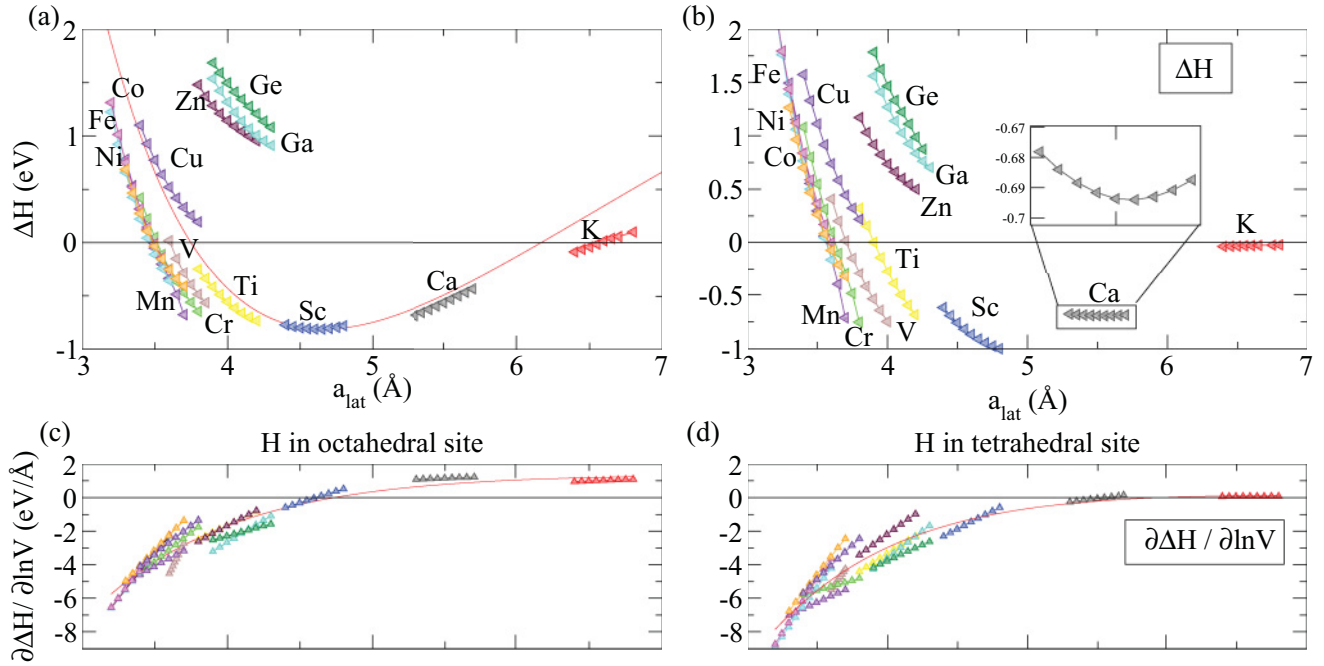


FIG. 2. (Color online) Solution enthalpy ΔH for: hydrogen in o-site (a) and in t-site (b). Furthermore the derivative of the solution enthalpy ΔH with respect to the logarithmic volume for hydrogen in the o-site (c) and hydrogen in the t-site (d) is shown. The red line indicates a fit of the resulting master curve of the simplified form $\Delta H(a_{\text{lat}}) = \alpha \exp(-a_{\text{lat}}) - \beta(1/a_{\text{lat}})$. The linear dependence of the derivative is due to the second-order fit of the ΔH values.

the volume enters, we fit for each element the discrete data [shown in Figs. 2(a) and 2(b)] to a third-order polynomial. The pressure dependence of the bulk modulus as well as the excess volume have been determined through the Murnaghan equation of state. The results are summarized in Fig. 3. As can be seen, the points are close to the analytical expression (solid red line). We therefore conclude from the validity of Eq. (8) that the universality described in (i) applies also to the product of the pressure-dependent bulk modulus and the excess volume, and less rigorously also to the individual quantities $B(p)$ and $V_H(p)$. The remaining part of the paper is devoted to understanding of the origin of the numbers and effects mentioned in (i) and (ii).

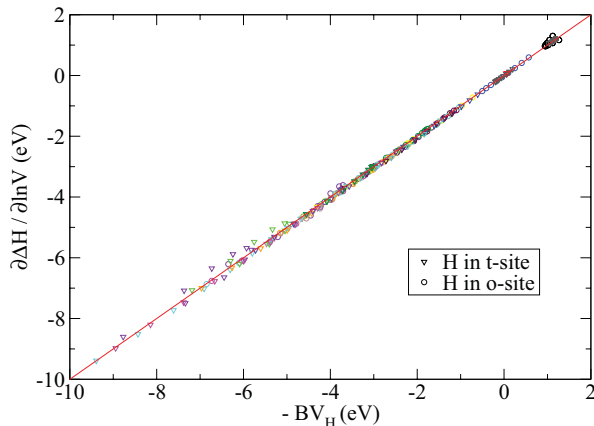


FIG. 3. (Color online) The derivative of the solution enthalpy as a function of the bulk modulus B multiplied by the excess volume V_H . The solid red line gives the analytical relation [see Eq. (8)].

C. Hard spheres model

In a first step, we focus on geometrical aspects and consider atoms to be hard spheres. If interstitial hydrogen is represented by a specific atomic radius, it needs a sufficiently large interstitial volume to allow an incorporation. An octahedron (tetrahedron) formed by hard spheres (situated at the corners and touching each other) has in its center some free space, which can be used to incorporate hydrogen (see Fig. 4).

By varying the lattice constant, the free volume in the octahedron is changing. If we assume that at a given lattice constant, the surrounding host atoms are touching each other, the hard sphere radius for the host atoms is then given by

$$r_{\text{host}}(a_{\text{lat}}) = a_{\text{lat}}/\sqrt{8}. \quad (11)$$

Based on this condition, the interstitial radius of a sphere that fits into the empty space in an o-site is then given by

$$r_{\text{Hocta}}(a_{\text{lat}}) = a_{\text{lat}}(\sqrt{2} - 1)/\sqrt{8}, \quad (12)$$

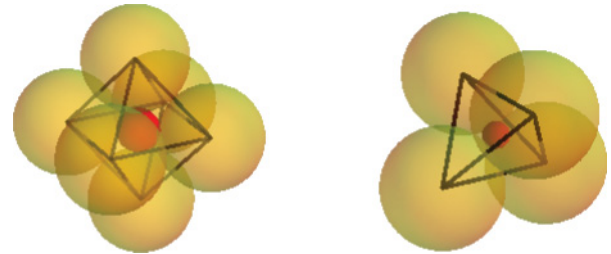


FIG. 4. (Color online) Hard spheres model: hydrogen (red) located in an o-site (a) at $a_{\text{lat}} = 4.6 \text{ \AA}$ and in a t-site (b) at $a_{\text{lat}} = 5.5 \text{ \AA}$ with host atoms (yellow) sitting at the octahedral (tetrahedral) corners.

and the interstitial radius in a t-site is given by

$$r_{\text{Htetra}}(a_{\text{lat}}) = a_{\text{lat}} (\sqrt{6} - 2) / \sqrt{32}. \quad (13)$$

Applying these formulas for the site-dependent optimum lattice constant ($a_{\text{lat}}^{\text{octa}} = 4.6 \text{ \AA}$ and $a_{\text{lat}}^{\text{tetra}} = 5.5 \text{ \AA}$), we obtain $r_{\text{host}}(a_{\text{lat}}^{\text{octa}}) = 1.6 \text{ \AA}$ and $r_{\text{host}}(a_{\text{lat}}^{\text{tetra}}) = 1.9 \text{ \AA}$. Using Eqs. (12) and (13), we find for the H radii $r_{\text{Hocta}}(a_{\text{lat}}^{\text{octa}}) = 0.7 \text{ \AA}$ and $r_{\text{Htetra}}(a_{\text{lat}}^{\text{tetra}}) = 0.4 \text{ \AA}$, i.e., both are significantly different. Interestingly, however, the host atom-H bond length in the o-site $r_{\text{host}}(a_{\text{lat}}^{\text{octa}} + r_{\text{Hocta}}(a_{\text{lat}}^{\text{octa}}))$ and in the t-site $r_{\text{host}}(a_{\text{lat}}^{\text{tetra}}) + r_{\text{Htetra}}(a_{\text{lat}}^{\text{tetra}})$ is for both sites approximately 2.3 \AA , i.e., independent on the site.

A smaller lattice constant yields a more dense ion packing, and leaves less space for hydrogen, resulting in a higher solution enthalpy, and higher enthalpy of solution, respectively. This argumentation is in agreement with the above mentioned investigation of Syono *et al.*, reporting about incompressibility of hydrogen in metals.⁶ Using high-pressure techniques, a similar observation of H incompressibility has been reported by Baranowski in an experimental study on H solubility in fcc metals.³¹ However, such a model does not explain why the solubility goes down when exceeding a critical lattice constant. Furthermore, as will be discussed below, the hard sphere model predicts for both sites (t and o) nonidentical sphere radii for the H atom.

We have checked the validity of the o-site minimum at 4.6 \AA and the t-site minimum at 5.5 \AA for the elements Ca, Sc, Ti, Mn, Fe, Cu, Zn, Ga, and Ge. Since the lattice constant for most of these elements is much smaller (or higher) a giant tensile (compressive) strain occurs when probing the minimum of the master curve. As a result, these structures become unstable when introducing H. To avoid this instability, we enforce for the host atoms the ideal fcc structure (no relaxations). In the o-site, the resulting optimum lattice constant for Ca, Zn, and Ti coincides with that of Sc (i.e., is consistent with a hydrogen radius of approximately 0.7 \AA in the hard sphere model). In the case of Mn, Fe, and Cu, the optimum lattice constant is with approximately 4.1 \AA (compared to 4.6 \AA), which is slightly smaller. The highest resulting optimum lattice constant has been achieved for the elements Ga and Ge with approximately 5.3 \AA . The resulting hard sphere radius for the interstitial in an o-site is between the range from 0.6 to 0.77 \AA .

For H in t-site, we find a slightly different trend for the optimum lattice constant. The resulting hard sphere radius is in the range from 0.35 to 0.44 \AA and thus much smaller. We therefore conclude that a value between 0.6 and 0.77 \AA (0.35 to 0.44 \AA) is an optimum chemical interaction radius for hydrogen in an o-site (t-site).

Recent *ab initio* studies on hydrogen-vacancy interaction in fcc iron revealed that it is energetically more favorable for hydrogen to be situated in the $\langle 100 \rangle$ directions from the vacancy center. The (high-symmetric) vacancy center itself is a local maximum and not preferable for hydrogen.³² An interesting question is whether the H-M binding is strong enough to break (o-site) symmetries in crystals where the lattice constant is larger than 4.6 \AA . This can be realized, e.g., by shifting the H atom away from the interstitial center. For this purpose, we made test calculations for H in Ca, since the lattice constant of Ca is well above the minimum one. To break the symmetry, we position a H atom off center at a distance

of 2.3 \AA of a single Ca atom (of two Ca atoms, respectively). Performing atomic relaxations, the H atom moves back into the high-symmetry o-site. Thus, for all elements studied here, the qualitative character when going from a compressed to a tensile interstitial configuration remains unchanged and provides the basis for the universal shape of the master curve.

D. Separation of strain and chemical effects

The strong impact of the lattice constant on H solubility can have various physical origins. It is straightforward to assume that atomic relaxation effects are critical. To estimate their importance, we decompose the solution energy into its various contributions. The strain energy ΔE_{strain} is the energy difference between the two different configurations of the matrix atoms (without hydrogen):

$$\Delta E_{\text{strain}} = E_{\text{M}_N/\text{H}_1}^{\text{relaxed}} - E_{\text{M}_N}^{\text{ideal}}. \quad (14)$$

Here, the term $E_{\text{M}_N/\text{H}_1}^{\text{relaxed}}$ describes the relaxed positions of the host atoms due to the incorporation of H (total energy without hydrogen) and the second term describes the ideal fcc lattice positions. The remaining part of the H solution enthalpy at the right-hand site of Eq. (3) is called chemical effect and given by

$$\Delta E_{\text{chem}} = E_{\text{M}_N/\text{H}_1}^{\text{relaxed}} - E_{\text{M}_N/\text{H}_1}^{\text{relaxed}} - \frac{1}{2} E_{\text{H}_2}. \quad (15)$$

The results are shown in Fig. 5.

The energy gain due to relaxation effects is by definition always positive. In the case of H in an o-site [see Fig. 5(a)] it shows a remarkable dependence on the lattice constant. When going away from the optimum lattice constant toward smaller ones, the expected increase of (compressive) strain energy is seen. Also toward the opposite limit of larger lattice constants, an equally strong increase of (in this case tensile) strain energy is observed, i.e., the host atoms neighboring H are pulled toward the impurity. It is remarkable that the minimum, where the strain energy vanishes, is close to the optimum lattice constant of the master curve. This configuration may thus be regarded as special in the sense that no displacements of matrix atoms are necessary when H is included. The increase of compressive energy is approximately two times larger in the case of H in t-site [see Fig. 5(c)]. The stronger relaxation in the t-site can partly be explained by the smaller hydrogen-metal distance for the identical lattice constants.

In this context it is, however, surprising that for the t-site the optimum lattice constant with respect to strain energy also seems to be around 4.6 \AA , whereas the minimum solution enthalpy occurs at around 5.5 \AA . This observation indicates the limitations of a simple geometrical sphere model in describing solution of hydrogen. One reason for the obvious limitations may be that the model does not consider second-nearest neighbors. A direct comparison between the o-site and t-site is also difficult because of geometric differences between these sites. Employing a Voronoi construction to determine interstitial volumes, we observe that the hydrogen atom sitting in an o-site is completely surrounded by octahedral atoms, whereas the hydrogen atom in the t-site has a contact surface to the second NN atoms. Eventually, the number of chemical bonds is influenced by this coordination effect. The importance of such chemical coordination effects becomes particularly

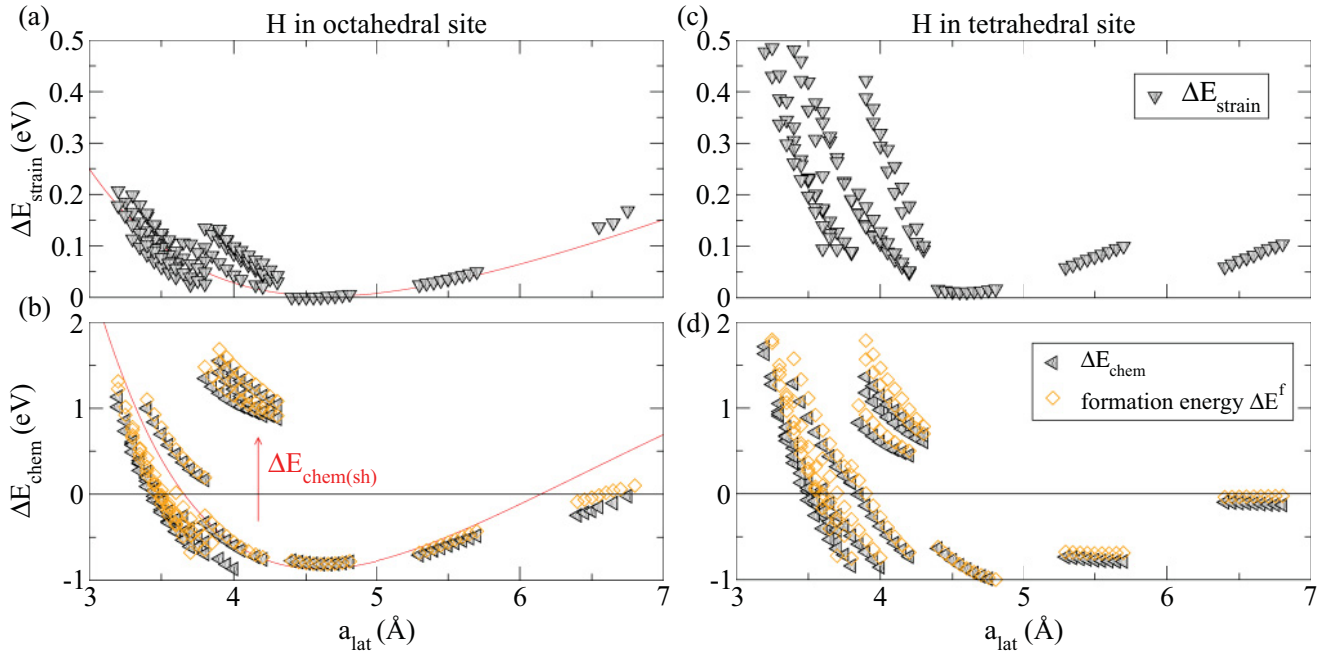


FIG. 5. (Color online) Separation of the solution enthalpy into a strain (a) and a chemical part (b) for o-sites. The strain energy is determined by relaxation effects of the host matrix whereas the chemical energy is determined by the interaction of the H atom with the matrix atoms. Both energy curves show an approximate master curve of the form $\alpha \exp(-a_{\text{lat}}) - \beta(1/a_{\text{lat}})$ (red). For H in the t-site, the same separation into a strain (c) and a chemical part (d) is given.

clear when noticing that in both cases ΔE_{strain} is almost an order of magnitude smaller than ΔE_{chem} , i.e., the solution enthalpy curve ΔH is mainly determined by ΔE_{chem} . We therefore conclude that the universal master curve is not dominated by H induced strain in the host lattice, but rather by the strength of the H-metal bonds.

E. Zero-point vibrations

An effect, which might be particularly relevant for a light weight element such as hydrogen, is the change of the solution enthalpy due to zero-point vibrations (ZPE). We have therefore studied this contribution for H in different elements and different sites employing the two methods introduced in Sec. IIC. The Einstein method is the computationally much faster but also more approximate method to compute ZPE. We have used the Einstein method to calculate the volume dependent contribution of the ZPE for H in Sc (o-site) and in Ca (t-site). The lattice constants of these two materials have been changed such that a compressive, respectively, a tensile, strain up to 5% was achieved. It turned out that for both elements, the energy difference between the tensile and compressive regions of the material does not exceed a total value of 50 meV.

A more accurate method is the calculation of the full dynamical matrix. The results of the latter method can be seen in Fig. 6. For the missing matrix elements, V, Cr, Ni, and Ge imaginary frequencies were obtained. Imaginary frequencies indicate that these elements are unstable in an fcc structure. Nevertheless, a calculation of the hydrogen ZPE in these elements was still possible within the Einstein method. For the elements Zn and Ga, we obtained imaginary frequencies

for H in the o-site. We notice a trend of the ZPE with respect to the d -band filling. With the filling of the d band the ZPE energy is increasing linearly until it reaches a maximum at a half-filled d band. With further filling of the d band the ZPE energy is decreasing linearly. Again, we observe a clear dependence with respect to the host lattice constant. Two observations are noteworthy: first, the results are largely independent with respect to the particular site chosen by the H atom. Second, the effect of the ZPE on the solution enthalpy vanishes almost completely at the previously identified specific lattice constant of 4.6 Å. We note that the highest effect on

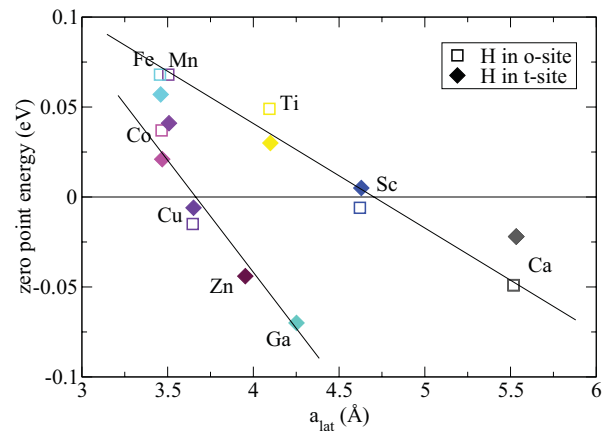


FIG. 6. (Color online) Effect of hydrogen zero-point Energy (ZPE) on the solution enthalpy. The ZPE are calculated within the harmonic approximation. Open squares: H in o-site, filled diamonds: H in t-site. For some host elements (V, Cr, Ni, Ge) not shown in this figure, imaginary frequencies (see text) were obtained.

the solution enthalpy due to zero-point vibrations is less than 0.08 eV. Including ZPE will therefore affect chemical trends only moderately. In fact, the zero-point energies are well below our targeted convergence criterion (0.15 eV).

F. Chemical shift of ΔH

For chemical elements, which have similar lattice constants the chemical offset in solution energies can be obtained. As shown in Figs. 2(a) and 2(c), the slope of ΔH is independent on the specific element. The offset in the absolute value of the solution enthalpy is thus a direct consequence of the specific chemical nature of the host-hydrogen interaction. A general observation is that elements with filled d shells (e.g., Zn, Cu, Ga, Ge) have a higher solution enthalpy than elements without filled $3d$ shells (e.g., Ti, Fe, V). The filling of the $3d$ shell is not directly correlated with the lattice constant, see e.g., Zn and Ti in Fig. 2.

When discussing the chemical nature of the unperturbed host lattice, previous works^{11,12} mainly considered global electronic properties of the pure bulk system (ΔE and W_d) as the relevant quantities influencing the hydrogen solubility. In these studies, the analysis of the electronic density of states (DOS) plots revealed that the difference in the global electronic structure between dilute hydrogen and the pure metallic systems is not significant. Locally, however, hydrogen dissolved in the metal is expected to accumulate charge close to its shell.⁴ We therefore focus on local effects around the H atom and analyze the hydrogen induced perturbation of the electronic charge by considering electronic charge density differences (CDD) between the perturbed and unperturbed systems. The difference is given by the equation

$$n(r)_{\text{CDD}} = n_{\text{M,H}}^{\text{relaxed}}(r) - n_{\text{M}_x}^{\text{relaxed}}(r) - n_{\text{H}}(r) \quad (16)$$

in which the first part describes the electronic charge of the metal-hydrogen system. The second part belongs to the metallic system, with the positions of the metal atoms being identical to the M-H system. The last part is the electronic charge of a single hydrogen atom in vacuum. For Ti, the CDD isosurface is shown in Fig. 7. The analysis of the isosurfaces revealed for all elements an isotropic charge accumulation at the H position. For a more quantitative evaluation, a 2D intersection for all elements is shown in Fig. 8. The pronounced maximum observed for all elements in Fig. 8 is the result of the attractive Coulomb interaction of the proton. As can be seen, the amount of accumulated electronic charge at the hydrogen atom depends on the specific host element. Elements on the left side of the periodic system with a low number of $3d$ electrons like Ca, Sc, and Ti show a higher perturbation of the electronic charge, induced by hydrogen. Elements to the right, like Cu, Zn, and Ge, with closed $3d$ shells, have a lower perturbation of the electronic charge. This behavior can be understood within a bonding (*anion model*) picture: hydrogen minimizes its energy by binding an extra electron in its $1s$ shell. Transition metals with incompletely filled $3d$ shells have thus a higher tendency to donate electrons.

According to the proton model,⁴ an additional electron (coming from H) will be added at the Fermi level, the Coulomb interaction of electrons will increase with higher electron densities, and as a consequence an increase of ΔH follows.

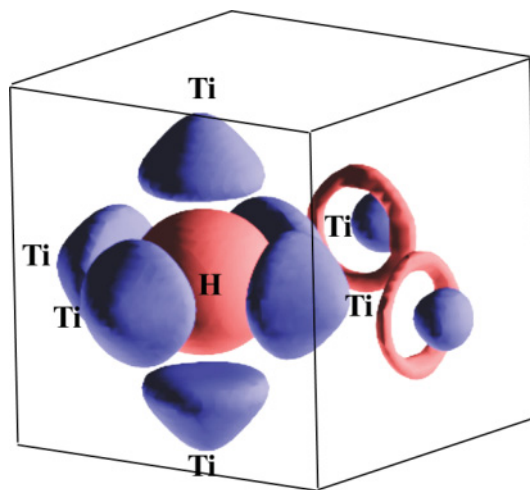


FIG. 7. (Color online) Isosurface for the charge density difference $n_{\text{CDD}}(r)$ using the example of Ti. The electron accumulating region (H position) is red coded and the donating region (host atoms) blue. For all elements, the electronic accumulation at H is isotropic.

This is related to the higher electronic density of states at the Fermi level for elements with filled $3d$ shells as compared to early transition metals. In this study, the change of the states at the Fermi level was not observed. However, based on the results shown in Fig. 8, for dilute hydrogen in $3d$ metals, the solution energy actually increases with the CDD (charge accumulation) at the H position. Furthermore, the s -like state was occupied with two electrons in almost all studied elements, i.e., the anion model⁴ seems to be a much more appropriate model for dilute hydrogen.

A more quantitative analysis is given in Fig. 9. In Fig. 9(b), ΔE_{chem} is plotted against the spherically integrated CDD (see Fig. 8). The radius of the integration sphere is determined by the transition point from negatively to the positively charged CDD. We observe a clear correlation: a larger CDD is related to a reduced ΔE_{chem} . Therefore H solubility increases with the ability of the host to donate electrons to H. The correlation becomes much clearer if the shift of the chemical energy $\Delta E_{\text{chem}}(\text{sh})$, which is the energy difference between ΔE_{chem} and the master curve in Fig. 5, is considered. The result is

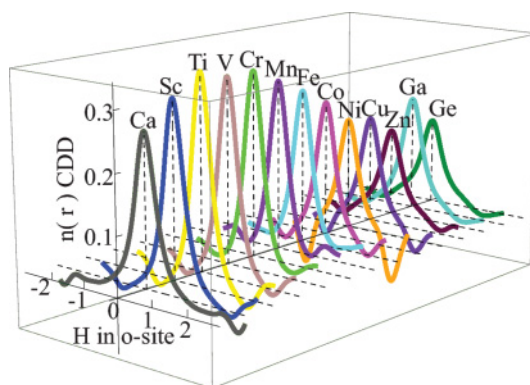


FIG. 8. (Color online) 2D intersections through the charge density difference between the systems with and without hydrogen for different elements. For H in an o-site, a positive peak for all elements is seen and the electronic charge is increased.

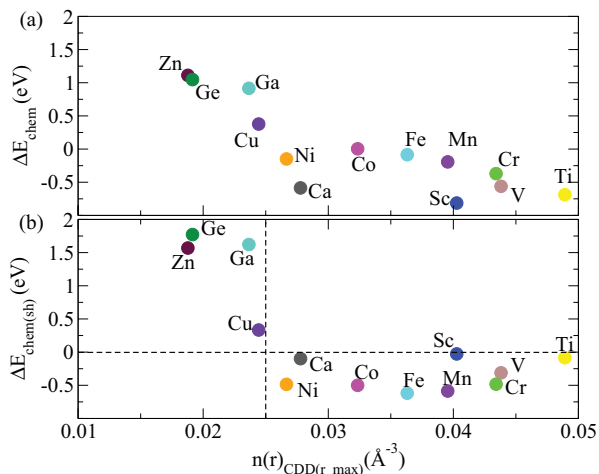


FIG. 9. (Color online) Chemical effect as a function of the spherically integrated CDD (see text). (a) The chemical effect vs the integrated CDD. Early elements of the transition series (Sc, Ti, V, Cr, Mn) show larger polarization effects. Such screening effects lower the chemical offset and simultaneously increase H solubility. (b) The element dependent chemical shift relative to the master curve vs the integrated CDD. The plot reveals a critical value of CDD for the elements, which separates the studied elements in two classes.

plotted in Fig. 9(a) versus the spherically integrated CDD. Here, a critical value of 0.025 electrons/ \AA^3 for the CDD is obtained, which separates the elements into two classes: all transition metals except Cu and Zn have a CDD larger than the critical value, which results to a ΔE_{chem} below the master curve. The elements Cu, Zn, Ga, and Ge, on the other hand, in which H is less soluble are below the critical CDD value.

G. Comparison with previous approaches

In the following section, we compare our *ab initio* evaluation with previously suggested approaches to assess ΔH . According to Griessen *et al.*, ΔH can be expressed for d metals as an approximate function of various physical quantities (ΔE , W_d , and R_j) of the unperturbed host system. In the following, we derive these quantities from our method for the $3d$ metal and check at the same time the extendibility to other metals considered in this work.

The energy difference between the Fermi level and the center of the lowest-lying conduction band, $\Delta E = E_F - E_s$, is a global parameter describing the structure of the undisturbed crystal. In order to determine its *ab initio* value, we have integrated the electronic density of states (DOS) of the pure bulk system. The way to determine the center of the lowest lying (s -like) conduction band E_s is discussed in Ref. 11: E_s is the energy for which the integrated DOS is equal to one and E_F is simply the energy at the Fermi level.

According to Eq. (9), the choice of the chemical element affects with ΔE , W_d , and R_j three quantities simultaneously. Thus to evaluate the validity of Eq. (9), we take the dependence on two of these quantities for granted and check the dependence on the third by rearranging Eq. (9) as, e.g., in the

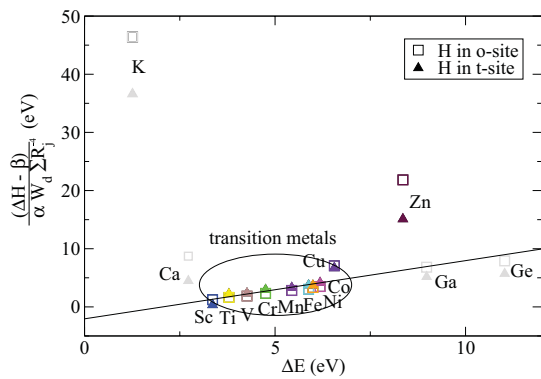


FIG. 10. (Color online) Correlation between Griessen's approach¹² for the H solution enthalpy and the parameter ΔE , as obtained from our *ab initio* calculations. Open squares: hydrogen in the o-site. Filled triangles: hydrogen in the t-site.

case of ΔE :

$$\frac{\Delta H - \beta}{\alpha W_d^{1/2} \sum R_j^{-4}} = \Delta E \quad (17)$$

(respectively rearranging the equation for W_d and R_j). Here, we take for the fitted parameters the values $\alpha = 0.13$ (eV/atom)(eV $^{-3/2}$ \AA^4) and $\beta = -1.07$ eV/atom. For the transition metals as predicted by the Griessen approach, there is a perfect correlation between the parameters since all values should lie on the black line (see Fig. 10). We see that the model can even be extended to Ga and Ge but not to the elements K, Ca, and Zn.

The analogous analysis is performed for the distance between interstitial hydrogen and the neighboring atoms R_j (see Fig. 11). Here again, the linear behavior is reproduced for the transition metals, and can be extended to Ga and Ge. The correlation between the Griessen parameter d -bandwidth W_d (which we have treated as the full bandwidth) and the rearranged Eq. (17) is shown in Fig. 12.

In conclusion, the Griessen parameters ΔE , W_d , and R_j , which can be easily obtained from *ab initio* calculations of the unperturbed host material, can be used to predict hydrogen solution in transition metals. The approach fails, for the studied alkali metals K and Ca and the late transition metal Zn.

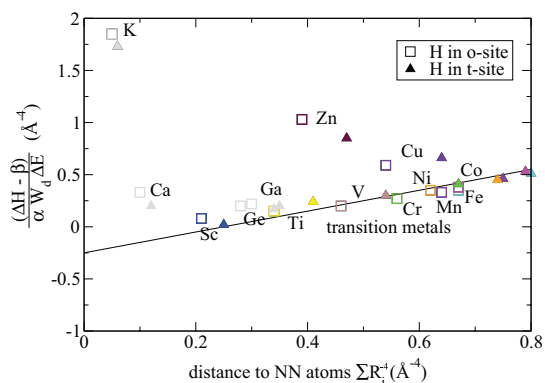


FIG. 11. (Color online) Correlation between Griessen's approach and the distance to NN atoms $\sum_j R_j$. Open squares: hydrogen in o-site. Filled triangles: hydrogen in t-site.

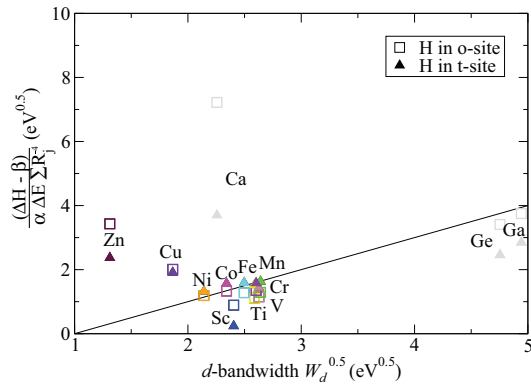


FIG. 12. (Color online) Correlation between Griessen's formula and the d bandwidth W_d . Open squares: hydrogen in the o-site. Filled triangles: hydrogen in the t-site.

However, we found that it can be extended to Ga and Ge, which have like Zn a full $3d$ shell.

IV. CONCLUSION

Using DFT and a large set of metals we identified chemical trends for the solution enthalpy ΔH of interstitial H. To ensure a systematic comparison, we restricted the study to (i) $3d$ transition metals and the neighboring elements K, Ca, Ge, and Ga, (ii) the fcc crystal structure, and (iii) nonmagnetic configurations. The ability of the *ab initio* approach to implement these constraints, is a clear advantage compared to previous empirical studies that were solely based on experimental data.

Systematically using these constraints, we were able to identify several rules for hydrogen solubility in transition metals. (1) Most importantly, our results reveal a hitherto not expected universal behavior between the hydrogen solution enthalpy versus lattice constant of the host metal. The universality becomes most apparent if strained materials are considered. (2) The solution enthalpy is the result of a competition between sufficient space to incorporate hydrogen (i.e., a preference for large lattice constants) and the formation of strong hydrogen-metal bonds (favoring smaller atomic distances). The first trend is consistent with previous observations in the Fe-Mn system.¹³ In the present study, we identified an

optimal spherical radius for interstitial H of approximately 0.7 \AA in the octahedral site (0.4 \AA in the tetrahedral site, respectively). (3) An fcc-lattice constant of 4.6 \AA turned out to be characteristic for several atomistic mechanisms. In particular, at this lattice constant, no relaxation of matrix atoms is needed upon hydrogen incorporation at the octahedral site. (4) These observations motivate a decomposition of the hydrogen solution enthalpy in a strain-induced part ΔE_{strain} (related to the lattice relaxations) and a remaining chemical part ΔE_{chem} . (5) Such defined chemical part, ΔE_{chem} , contains the energy related to the formation of chemical bonds. It covers the largest part of the hydrogen solution enthalpy. Accordingly, its volume dependence also shows the universal behavior observed for the whole solution enthalpy. (6) Investigating charge density differences at the hydrogen position revealed two classes of elements: in one class only a small part of the electronic charge of the matrix material is locally bound at the hydrogen position. This is a consequence of the limited ability of these materials to screen the proton. The resulting reduction in ionic character explains the significantly higher endothermic hydrogen solution enthalpy.

The above insights were only possible due to the *ab initio* nature of this study, which allowed to assess earlier, more empirical findings for the dependence of the hydrogen solution enthalpy in metals. We found that the parameters suggested in the work of Griessen¹² for transition metals yield trends that are reasonably confirmed by our *ab initio* data and can even be extended to further fourth row elements like Ga and Ge.

Despite the approximations in the DFT exchange-correlation functionals used in our approach, the good agreement with experimental data makes us confident that our predictions are qualitatively correct. Besides the achieved general understanding of fundamental rules for the incorporation of interstitial hydrogen, we believe that the knowledge of such trends may help in understanding and designing materials where dilute H concentration have severe effects on functionality and/or structural solubility such as, e.g., H embrittlement.

ACKNOWLEDGMENTS

Special thanks go to R. Nazarov, J. Pezold, and F. Koermann for fruitful discussions and comments.

*u.aydin@mpie.de

¹T. Graham, R. Soc. **156**, 399 (1866).

²R. Oriani, *Ann. Rev. Mater. Sci* **8**, 327 (1978).

³C. Lundin, F. Lynch, and C. Magee, *J. Less-Common Met.* **56**, 19 (1977).

⁴A. C. Switendick, *The Change in Electronic Properties on Hydrogen Alloying and Hydride Formation* (Springer, Berlin, Heidelberg, 1978).

⁵C. D. Gelatt, H. Ehrenreich, and J. A. Weiss, *Phys. Rev. B* **17**, 1940 (1978).

⁶Y. Syono, K. Kusaba, K. Fukuoka, Y. Fukai, and K. Watanabe, *Phys. Rev. B* **29**, 6520 (1984).

⁷J. Hirth, *Metall. Mater. Trans. A* **11**, 861 (1980).

⁸J. Nørskov and F. Besenbacher, *J. Less-Common Met.* **130**, 475 (1987).

⁹V. Shivanyuk, V. G. Gavriljuk, and J. Foct, *Mater. Sci. Forum* **539–543**, 4249 (2007).

¹⁰A. Miedema, K. Buschow, and H. V. Mal, *J. Less-Common Met.* **49**, 463 (1976).

¹¹R. Griessen and A. Driessen, *Phys. Rev. B* **30**, 4372 (1984).

¹²R. Griessen, *Phys. Rev. B* **38**, 3690 (1988).

¹³L. Ismer, T. Hickel, and J. Neugebauer, *Phys. Rev. B* **81**, 094111 (2010).

¹⁴H. Wipf, *Phys. Scr.* **T94**, 43 (2001).

¹⁵R. Griessen and R. Feenstra, *J. Phys. F* **15**, 1013 (1985).

¹⁶F. Murnaghan, *Natl. Acad. Sci. USA* **30**, 244 (1944).

- ¹⁷B. Grabowski, T. Hickel, and J. Neugebauer, *Phys. Rev. B* **76**, 024309 (2007).
- ¹⁸P. E. Blöchl, *Phys. Rev. B* **50**, 17953 (1994).
- ¹⁹G. Kresse and J. Furthmüller, *Phys. Rev. B* **54**, 11169 (1996).
- ²⁰J. P. Perdew, K. Burke, and M. Ernzerhof, *Phys. Rev. Lett.* **77**, 3865 (1996).
- ²¹H. J. Monkhorst and J. D. Pack, *Phys. Rev. B* **13**, 5188 (1976).
- ²²M. Methfessel and A. T. Paxton, *Phys. Rev. B* **40**, 3616 (1989).
- ²³R. Griessen and R. Riesterer, *Heat of Formation Models* (Springer, Berlin, Heidelberg, 1988).
- ²⁴E. Fromm and G. Hörz, *Intern. Metals Rev.* **15**, 269 (1980).
- ²⁵M. Nagasaka and T. Yamashina, *J. Less-Common Met.* **45**, 53 (1976).
- ²⁶H. Behrens and G. Ebel, in *Physica Data Series 5* (Fachinformationszentrum Energie, Physik, Mathematik, Karlsruhe).
- ²⁷A. Driessen, H. Hemmes, and R. Griessen, *Z. Phys. Chem.* **143**, 145 (1985).
- ²⁸C. Papastaikoudis, B. Lengeler, and W. Jager, *J. Phys. F* **13**, 2257 (1983).
- ²⁹E. Fromm and E. Gebhardt, *Gase und Kohlenstoff in Metallen* (Springer, Berlin, Heidelberg, 1976).
- ³⁰R. Frank and J. Thomas Jr., *J. Phys. Chem. Solids* **16**, 144 (1960).
- ³¹B. Baranowski, S. Majchrzak, and T. B. Flanagan, *J. Phys. F* **1**, 258 (1971).
- ³²R. Nazarov, T. Hickel, and J. Neugebauer, *Phys. Rev. B* **82**, 224104 (2010).